NEUTRON SCATTERING STUDY OF ANTIFERROMAGNETIC CORRELATIONS IN THE Zn-Mg-Ho ICOSAHEDRAL QUASICRYSTAL

Taku J. SATO*, Hiroyuki TAKAKURA*,**, An Pang TSAI*, Kaoru SHIBATA***, Kenji OHOYAMA*** and Ken H. ANDERSEN****

*National Research Institute for Metals, Tsukuba 305-0047, Japan
**CREST, Japan Science and Technology Corporation, Kawaguchi, Saitama, Japan
***Institute for Materials Research, Tohoku University, Sendai, Japan
****Institute Laue Langevin, Grenoble, France

ABSTRACT

Magnetism in the Zn-Mg-Ho icosahedral quasicrystal has been studied by neutron scattering. Powder samples of the icosahedral and related crystalline phases were reexamined to clarify the origin of the previously-reported long-range magnetic order [Charrier *et al.*, Phys. Rev. Lett. **78** (1997) 4637]. The long range order was found to originate from the related crystalline phase, which is a contaminant in the previously-used samples. Whereas for high-quality icosahedral phase, we could detect only magnetic diffuse scattering. This apparently shows the absence of the long range order in the icosahedral phase. The diffuse scattering was studied in detail by using a single quasicrystalline sample. It was found that the diffuse scattering appears as satellites from intense nuclear Bragg reflections. This indicates that corresponding spin correlations can be regarded as developed between spins on the six-dimensional virtual hypercubic lattice. A magnetic modulation vector for the correlations is proposed as $\vec{q}_{\mathrm{m}}^{\,6\mathrm{D}} = (\frac{3}{4}, 0, 0, \frac{1}{2}, \frac{3}{4}, \frac{1}{2})$.

INTRODUCTION

Since the discovery of a quasicrystal in the rapidly solidified Al-Mn alloy [1], magnetism of quasicrystals has been a fundamental issue to study. To date, quasicrystals were mainly found in the aluminum-based alloys, and thus great efforts were devoted to elucidate the magnetism on the alloys, such as Al-Pd-Mn [2, 3] and Al-Cu-Fe [4]. In those systems, possible origin of magnetic moments is d electrons of the transition metal elements. However, since they are itinerant or non-localized electrons, formation of the moments is not trivial, and is strongly affected by local environment, carrier density, and so on. This complexity prohibits us to reach a deep understanding of the magnetic behavior of those aluminum-based alloys. Recently, icosahedral quasicrystals were discovered in the Zn-Mg-RE (RE = rare earth) system with RE = Y, Gd, Tb, Dy, Ho and Er [5]. These quasicrystals are quite unique among existing ones since they have well-localized and sizable 4f magnetic moments on the RE sites. This characteristic provides us an opportunity to study a rather simple problem; behavior of the well-defined spins on quasiperiodic lattice.

To date, magnetism of the Zn-Mg-RE icosahedral quasicrystals has been studied by several groups. Hattori *et al.* [6], and Charrier and Schmit [7] reported results of magnetic susceptibility measurements. For the Ho system, the susceptibility shows paramagnetic increase as temperature is decreased until $T \simeq 10$ K, which can be well represented by the Curie-Weiss law with the magnetic moment of Ho^{3+} free ion. It starts to deviate from the Curie-Weiss line below about 10 K, however, the difference is very small, suggesting very

faint development of the magnetic correlations, and/or crystal-field splitting of about 10 K $\sim$ 1 meV. Then, it abruptly shows a spin-glass like irreversibility below $T_{SG} = 2$K. From those susceptibility data, the icosahedral Zn-Mg-Ho quasicrystal was suggested to be a typical spin-glass system with spins almost-randomly frozen.

In contrast, powder neutron scattering study reported a rather puzzling coexistence of the long-range and short-range magnetic order [8]. The magnetic diffuse and Bragg scattering starts to develop at the same temperature of $T_N \simeq 7$ K, which is higher than the spin-glass-like transition temperature T_{SG}. If the magnetic long-range order is established at T_N, then it must leave an anomaly in the susceptibility. However, in the susceptibility data we cannot see any anomaly, and thus those two experiments are contradicting.

Recent metallographic investigations show that the icosahedral quasicrystals has an almost stoichiometric composition of $Zn_{60}Mg_{30}RE_{10}$ [9, 10]. However, the previous neutron experiment used $Zn_{50}Mg_{42}RE_8$ samples, which can probably be contaminated by several crystalline phases. Therefore, reexamination of a high-quality single-phased sample is necessary. To study the magnetic correlations in detail, neutron scattering using a single quasicrystal is most preferable since it gives $\vec{Q}$-direction dependence of spin correlations. Further, a single quasicrystal is, in concept, free from the crystalline contamination, and thus we can reveal intrinsic nature of the magnetic ordering in the quasicrystal without confused by signals from contaminants.

In the present study, we have performed single-crystal growth of the Zn-Mg-Ho icosahedral quasicrystal. We have, then, carried out neutron scattering experiments on the single quasicrystalline sample, together with powder samples of quasicrystalline and related crystalline phases. The powder experiments clearly show that the previously-reported long-range order originates from the crystalline contamination. The icosahedral phase shows only well-developed diffuse scattering at the lowest temperature of $T \simeq 1.5$ K. The single crystal neutron scattering exhibits that the diffuse scattering appears as satellites from the intense nuclear Bragg reflections. This implies that a magnetic modulation vector for the diffuse scattering is defined in the six-dimensional (6D) hypercubic lattice. To confirm this, we applied the projection method to the magnetic diffuse scattering and succeeded to reproduce the observation qualitatively with the modulation vector of $\vec{q}_m^{\,6D} = (\frac{3}{4}, 0, 0, \frac{1}{2}, \frac{3}{4}, \frac{1}{2})$. For single quasicrystal growth, our report has been published in Ref. [11], whereas the results from other groups can be found in Refs. [12, 13]. Part of the neutron scattering study has already been published in Ref. [14], whereas complementary information on the different RE system appeared in literature, recently [15]. Details of this report will be published elsewhere [16].

EXPERIMENTAL

The power samples of $Zn_{60}Mg_{30}Ho_{10}$, $Zn_{50}Mg_{42}Ho_8$ and $Zn_{68}Mg_{16}Ho_{16}$ ($(Zn_{0.8}Mg_{0.2})_5Ho$) were prepared by melting constituent elements. The purities of the starting materials were 99.9999%, 99.99% and 99.9% for Zn, Mg, and Ho, respectively. The samples were then annealed under several conditions and characterized by scanning and transmission electron microscopies (SEM and TEM) and X-ray diffraction. Compositions of phases in the samples were determined by measuring energy-dispersive X-ray spectra in the SEM. Typical errors were Zn: ± 1.5 at.%, Mg: ± 3 at.% and Ho: ± 0.5 at.%. The single quasicrystal of $Zn_{60}Mg_{31}Ho_9$ was obtained by the Bridgeman method from the incongruent melt of $Zn_{46}Mg_{51}Ho_3$. Details of the crystal growth were published elsewhere [11].

The powder samples were mounted in a standard ^{4}He refrigerator and cooled down to

$T \simeq 1.3$ K. The single quasicrystal was also mounted in the same refrigerator with its two-, three- or five-fold (2f, 3f or 5f) axis vertical so that the scattering plane coincides with the 2f, 3f, or 5f plane, respectively. The triple-axis spectrometer ISSP-GPTAS installed at JRR-3M, JAERI (Tokai), was used to measure scattering from the powder samples, and from the 2f plane of the single quasicrystal. The spectrometer was operated in the double-axis configuration. Collimations of 40'-80'-40' or 40'-80'-80' were employed for the magnetic scattering experiments, whereas tight collimations of 10'-20'-20' were used for the sample quality check. Incident neutrons of $k_{\rm i} = 2.67$ Å^{-1} were selected by a vertically-focusing pyrolytic graphite (PG) monochromator, and second harmonics was eliminated by the PG filter. For the 3f and 5f planes, experiments were performed at the multidetector diffractometer HERMES, installed at JRR-3M [17]. The incident neutrons of $k_{\rm i} = 3.45$ Å^{-1} were selected by a vertically-focusing germanium monochromator with 331 reflections used. The higher order harmonics are negligibly small for this diffractometer. Since the unpolarized neutron scattering gives superposition of nuclear and magnetic scattering, we separated the magnetic contribution by subtracting the high temperature data, taken at $T \simeq 20$ K, from the data at the lowest temperature, $T \simeq 1.5$ K. The scattering was measured in the doubled symmetrically-independent region for each plane, which will be indicated in the corresponding figure. Then, after confirming that the magnetic scattering satisfies symmetry requirements, we folded the data into the single region to increase statistical accuracy. Finally, the data were unfolded for all plane to see characteristics of the intensity distribution.

NOTATION AND TERMINOLOGY

Notation and terminology are sometimes confusing in quasicrystals, and thus we summarize briefly what we will use in the following sections.

The *parallel* (*external*, *physical*) space and *perpendicular* (*internal*, *complementary*) space are defined as usual [18, 19]. $\vec{Q}^{\rm 6D}$ denotes a vector defined with the 6D reciprocal lattice bases, i.e., in r.l.u., whereas $\vec{Q}_{\parallel}$ and $\vec{Q}_{\perp}$ are projected vectors into the parallel and perpendicular space, respectively, and in Å^{-1} unit. $\vec{Q}$ is used in place of $\vec{Q}_{\parallel}$ where the usage is not ambiguous. A 6D vector, $(\vec{Q}_{\parallel}, \vec{Q}_{\perp})$, will be denoted as $\vec{Q}_{\parallel\perp}$, which is also in Å^{-1} unit. *Real* space is used in opposite to the *reciprocal lattice* space, both for the 3D and 6D space. Further, to specify a point in obtained intensity-maps, we introduce a vector $\vec{Q}_{\rm HK}$, which is defined for each 2f, 3f or 5f plane with bases being two orthogonal vectors along the axes of the figure.

ORIGIN OF THE BRAGG PEAKS IN POWDER SAMPLES

First of all, we examined the microstructure of the $Zn_{50}Mg_{42}Ho_8$ sample prepared under the same condition as the previous work [7]: the as-cast sample was annealed at 873 K for 20 min and subsequently at 673 K for 48 h. Shown in Fig. 1 is the backscattered electron image of a mechanically polished surface taken in the SEM. It clearly shows the coexisting four phases as $Zn_{57}Mg_{33}Ho_{10}$, $(Zn_{1-x}Mg_x)_5Ho$ ($x \sim 0.2$), Zn_3Mg_7 and Mg. The first one is the icosahedral quasicrystal, whereas the others are the crystalline contamination. Among them, the icosahedral and $(Zn_{1-x}Mg_x)_5Ho$ phases include a large amount of Ho atoms. Therefore, we could expect that the previous neutron diffraction pattern can possibly be superposition of the magnetic signals from those two phases.

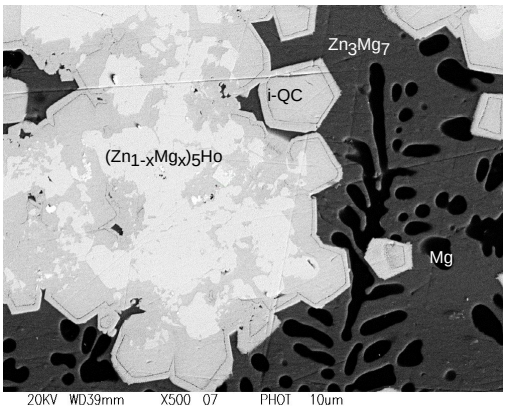

Figure 1: A backscattered electron image of a mechanically polished surface of the $Zn_{50}Mg_{42}Ho_8$ polycrystalline alloy. Coexisting four phases can be clearly seen.

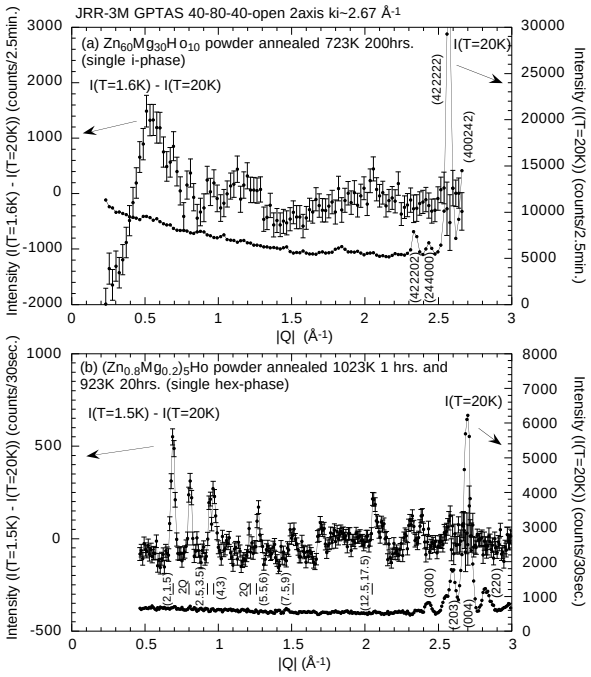

Figure 2: Neutron powder diffraction patterns for (a) the $Zn_{60}Mg_{30}Ho_{10}$ icosahedral phase and (b) the $(Zn_{1-x}Mg_x)_5Ho$ crystalline phase with $x = 0.2$. Subtractions, $I(T \simeq 1.6\text{K}) - I(T = 20\text{K})$, are shown as magnetic contributions. The vertical lines represent the intense long-range order peak-positions in the previous report with the proposed quasicrystalline indices [8]. Note that the magnetic Bragg peaks in (b) apparently originate from the crystalline phase.

Having the above metallographic knowledge in mind, we made a $Zn_{60}Mg_{30}Ho_{10}$ polycrystalline alloy. It was annealed at 723 K for 200 h to obtain a single icosahedral-phased sample. The powder neutron diffraction pattern is shown in Fig. 2(a). At the high temperature of $T = 20$ K, the system is in a paramagnetic state and the diffraction pattern only exhibits nuclear Bragg reflections, which can be well indexed with six-dimensional indices. The development of the magnetic scattering is shown by subtracting the high temperature paramagnetic data from the low temperature data at $T = 1.6$ K. Although the lower temperature is well below the reported ordering temperature of $T_{\rm N} \simeq 7$ K, there appear no magnetic Bragg peaks in the figure. Instead, the broad diffuse-scattering peaks can be seen in the figure at $Q \sim 0.55, 1.15, 2.0$ Å^{-1}, suggesting development of short range order.

The powder diffraction pattern of the crystalline $(Zn_{1-x}Mg_x)_5Ho$ sample with $x = 0.2$ is shown in Fig. 2(b) with the same manner as Fig. 2(a). The sample was annealed at 1023 K for 1 h and then at 923 K for 20 h for homogenization. The nuclear Bragg reflections can be indexed with hexagonal Zn_5Ho structure [20]. At low temperatures, magnetic Bragg peaks appear at the same positions as those in the previous report. In fact, they can be indexed with the quasicrystalline indices. However, this is misleading indexing, since they apparently originate from the crystalline phase. The transition temperature was determined as $T_{\rm N} \simeq 7.4$ K from magnetic susceptibility [16]. This coincides with the previously-reported $T_{\rm N}$ of the magnetic Bragg reflections in the $Zn_{50}Mg_{42}Ho_8$ sample. Those results clearly indicate that the magnetic Bragg reflections should be attributed to the crystalline phase,

and the intrinsic magnetism in the icosahedral quasicrystal is the short range order.

CHARACTERIZATION OF SINGLE QUASICRYSTAL

To reveal the nature of the short-range spin-correlations in the icosahedral quasicrystal, it is necessary to study $\vec{Q}$-dependence of the diffuse scattering in detail. Since a single quasicrystal is apparently required for this purpose, we have performed the single-crystal growth by the Bridgeman method [11]. The obtained single quasicrystal is shown in Fig. 3. The lower part is the single quasicrystalline precipitate, whereas the upper part mostly consists of the remaining binary (Zn-Mg) alloy. The volume of the single quasicrystal was about 0.5 cm^3. The quality of the obtained single quasicrystal was confirmed by X-ray, electron and neutron diffractions. Fig. 4(a-c) shows the X-ray back-reflection Laue photographs of the lower part. 2f, 5f and 3f symmetries are clearly seen in the figures. The 5f pattern in (b) was obtained by rotating the sample by 32° from the 2f axis along the 5f direction (shown in Fig. 4(a)), while the 3f pattern (c) by 21° along the 3f direction. Thus, the icosahedral symmetry is confirmed. The X-ray transmission Laue photograph is shown in Fig. 4(d), which was taken from a sphere-shaped sample with a diameter of about 250 μm. It shows a cherry-blossom-like pattern with a large number of sharp diffraction spots, and indicates the definite 5f symmetry.

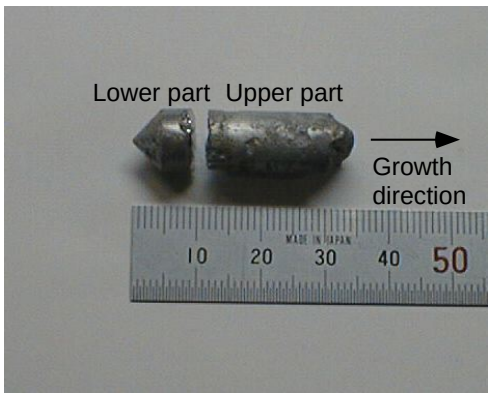

Figure 3: The grown rod of the Zn-Mg-Ho alloy obtained by the Bridgeman growth. (Lower part) Single crystal of the Zn-Mg-Ho icosahedral quasicrystal. (Upper part) Remaining Zn-Mg binary alloy.

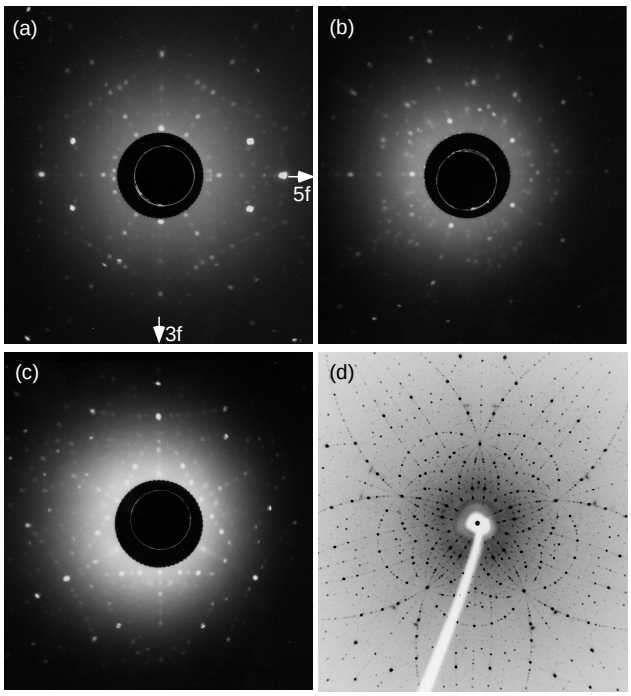

Figure 4: (a-c) X-ray back-reflection Laue photographs with X-ray along the (a)2f, (b)5f, and (c)3f axes. (d) An X-ray transmission Laue photograph along the 5f axis.

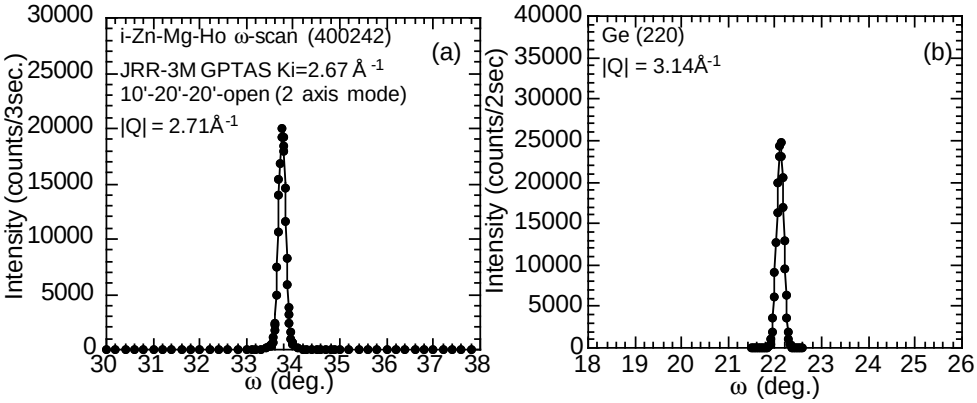

Figure 5: (a) An ω-scan around the 400242 reflection taken by the neutron triple-axis spectrometer. (b) An ω-scan around the 220 reflection of a standard germanium for comparison. The intrinsic mosaic spread of the standard germanium is negligibly small.

Overall quality of the sample was also checked by the neutron diffraction. An ω-scan around the 400242 reflection is shown in Fig. 5(a), with the whole lower-part in the neutron beam. Only one peak can be seen in the figure, indicating that the whole part is single-grained. The half-width at half-maximum (HWHM) of the peak is about 0.09°, which is comparable to the instrumental resolution of this configuration of the spectrometer. To see this, an ω-scan of the standard germanium 220 reflection is shown in Fig. 5(b). The intrinsic mosaic spread of the standard germanium is negligibly small for the neutron spectrometer. The HWHMs of the peaks are quite the same for both samples, indicating that the intrinsic mosaic spread of the single quasicrystal is also negligibly small.

MAGNETIC DIFFUSE SCATTERING IN THE SINGLE QUASICRYSTAL

Next, we investigated the $\vec{Q}$ dependence of the diffuse scattering using the single quasicrystal. Shown in Fig. 6 are results of $\vec{Q}$ scans along three symmetric axes in the first quadrant of the 2f plane, which are the 2f ($\vec{Q} \parallel (1,0,0)$), 3f ($\vec{Q} \parallel (\tau^2,1,0)$) and 5f ($\vec{Q} \parallel (1,\tau,0)$) axes. Magnetic intensity along the 2f axis, shown in Fig. 6(a), exhibits well-developed diffuse peaks, indicating the existence of the short-range spin-correlations. The correlation length was estimated as $\xi \sim 10$ Å from the diffuse-peak width of about $\gamma \simeq 0.1$Å^{-1} (HWHM) at $\vec{Q} = (0.55,0,0)$Å^{-1} on the 2f axis. Diffuse peaks could also be observed along the 3f axis, as shown in Fig. 6(b),with different peak positions. In contrast, the scan along the 5f axis, shown in Fig. 6(c), exhibits almost no magnetic contribution. Thus, modulation of the magnetic correlations in the Zn-Mg-Ho icosahedral quasicrystal is very anisotropic in $\vec{Q}$ space. This is in sharp contrast to glassy materials where correlations are isotropic and depend only on $|\vec{Q}|$. We further measured scans along the symmetrically equivalent directions, which are 2f ($\vec{Q} \parallel (0,1,0)$), 3f ($\vec{Q} \parallel (\tau^2,-1,0)$), and 5f ($\vec{Q} \parallel (-1,\tau,0)$) axes. They are in good agreement with the corresponding scans in the first quadrant, indicating the icosahedral symmetry of the diffuse scattering. Note that no magnetic Bragg reflections appear in the scans. This confirms the absence of the magnetic long-range order in the icosahedral quasicrystal.

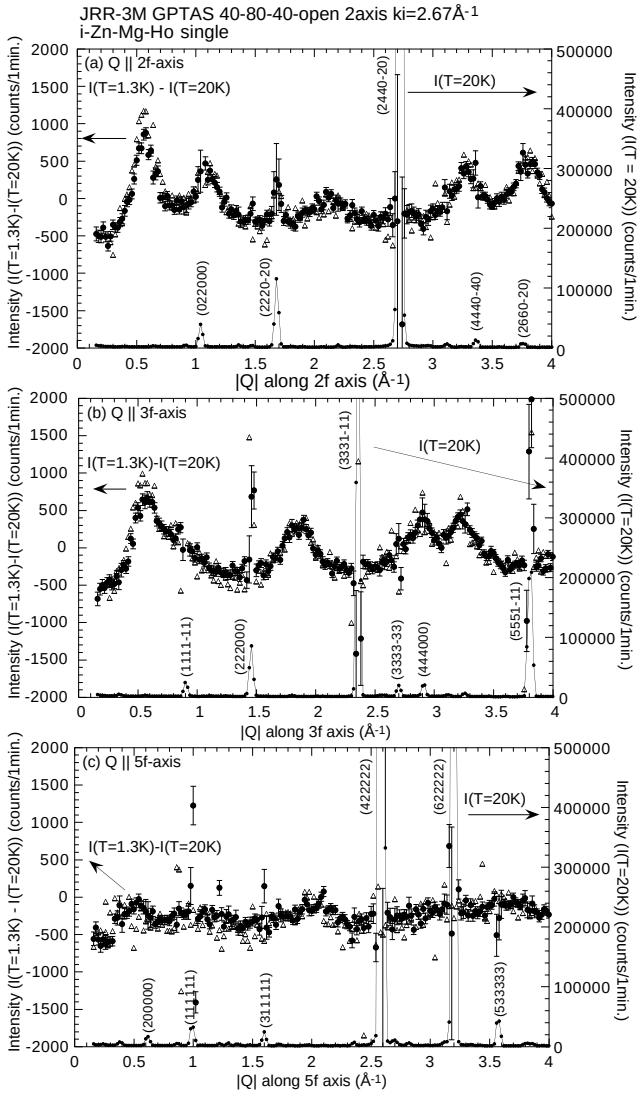

Figure 6: $\vec{Q}$ scans along the (a) 2f, (b) 3f and (c) 5f axes. Magnetic contributions were obtained by subtractions, i.e., $I(T = 1.3\text{K}) - I(T = 20\text{K})$. The sharp peaks observed at $T = 20$ K are the nuclear Bragg reflections, which are indexed with 6D indices.

To see overall features of the diffuse scattering apart from the symmetry axes, we have made magnetic-scattering intensity-maps in the 2f, 3f and 5f planes. The results are shown in the Fig. 7(a), 7(b) and 7(c), respectively. As described in the experimental section, we have measured the scattering only in doubled symmetrically-independent regions, which are shown in the figures by solid lines. In the figures, there appear a few spot-like peaks, which are, however, diffuse scattering as evidenced in Fig. 6. Positions of the intense nuclear Bragg reflections are denoted by white dots in the first quadrant of the figures, to relate the magnetic-scattering patterns to the Bragg reflections. One can see that the diffuse scattering appears where the intense nuclear Bragg reflections are absent. This confirms the antiferromagnetic nature of the spin correlations, first suggested from the susceptibility [6].

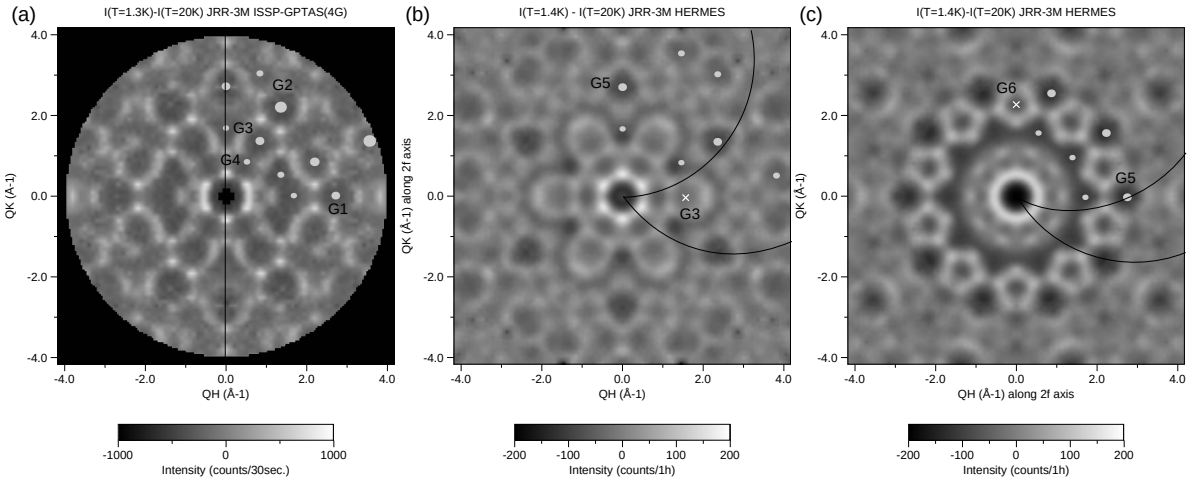

Figure 7: Magnetic diffuse-scattering intensity-maps for the (a) 2f, (b) 3f, and (c) 5f planes. The magnetic contributions were obtained by subtractions, i.e., $I(T \simeq 1.4\mathrm{K}) - I(T \simeq 20\mathrm{K})$. For the (a) 2f plane, half of the plane, $\vec{Q}_H > 0$, was measured, whereas for (b) 3f and (c) 5f planes, observation was made for regions between the two solid lines. White dots stand for the in-plane intense nuclear Bragg reflections in the first quadrant, whereas the white crosses are for the projected positions of the out-of-plane Bragg reflections, $\vec{G}_3^{\mathrm{6D}}$ and $\vec{G}_6^{\mathrm{6D}}$. Details are described in the text.

We, here, investigate details of magnetic scattering in each plane. In the 2f plane, one can see that the most intense diffuse scattering appears around the origin, $\vec{O}_{\parallel}$, with the distance of $|\vec{Q}_{\parallel}| \simeq 0.55\mathrm{Å}^{-1}$. The diffuse scattering is localized at $\vec{Q}_{HK} = (0, 0.55)$ Å^{-1}, whereas it is elongated along Q_K direction at $\vec{Q}_{HK} = (0.55, 0)$ Å^{-1}. This diffuse scattering pattern can be repeatedly recognized around the intense nuclear Bragg reflections, such as $\vec{G}_1^{\mathrm{6D}} = (2, 4, 4, 0, -2, 0)$, $\vec{G}_2^{\mathrm{6D}} = (4, 2, 2, 2, 2, 2)$ and $\vec{G}_3^{\mathrm{6D}} = (3, 1, 1, 1, 1, 1)$. This suggests that the magnetic diffuse scattering appears as satellites of the Bragg reflections in 3D reciprocal space. The positions of the satellites are given by $\vec{Q}_{\parallel} = \vec{G}_{\parallel} \pm \{\vec{q}_{\mathrm{m}\parallel}\}$, where $\{\vec{q}_{\mathrm{m}\parallel}\}$ denotes a set of symmetrically-equivalent modulation vectors. This set of equivalent vectors is necessary because short-range ordered domains with equivalent $\vec{q}_{\mathrm{m}\parallel}$ will be equally populated in general. A representative magnetic modulation-vector is inferred as $\vec{q}_{\mathrm{m}\parallel} = (0, 0.55, 0)$ from the localized peak on the Q_K axis. Equivalent vectors in the 2f plane are $(0.55, 0, 0), (-0.55, 0, 0)$ and $(0, -0.55, 0)$, which correspond to the satellites at $\vec{Q}_{HK} = (0.55, 0), (-0.55, 0)$ and $(0, -0.55)$ around the origin. The elongated feature can probably be explained by superimposing satellites of other reflections on those of the origin. For instance, a satellite of $\vec{G}_{4\parallel} - \vec{q}_{\mathrm{m}\parallel}$, where $\vec{G}_4^{\mathrm{6D}} = (1, 1, 1, 1, 1, 1)$, appears at $\vec{Q}_{HK} = (0.52, 0.29)$ Å^{-1}, which is on the elongated diffuse ridge at $Q_H = 0.55$ Å^{-1}. We should note that the intensities of the diffuse peaks at $\vec{G}_{\parallel} + \vec{q}_{\mathrm{m}\parallel}$ and $\vec{G}_{\parallel} - \vec{q}_{\mathrm{m}\parallel}$ are very different, for example, $I(\vec{G}_3 + (0, 0.55)_{\mathrm{HK}}) \neq I(\vec{G}_3 - (0, 0.55)_{\mathrm{HK}})$. This is in striking contrast to crystalline antiferromagnets where the satellite intensities are generally equal except for the form factor.

The diffuse peaks also appears on the six 2f-axes around the origin in the 3f plane. For the 5f plane, the ring-like appearance can be seen around the origin, which was confirmed to have peaks on the ten 2f-axes by the triple-axis spectrometer with high $\vec{Q}$-resolution. Since those two planes represent different sections of the $\vec{Q}_{\parallel}$ space, this confirms that the magnetic

modulation vector is localized on the 2f axis, as inferred from the 2f plane. The six-fold and ten-fold appearances of the peaks can originate from the domains with symmetrically-equivalent $\vec{q}_{\rm m}$. Around the intense Bragg reflection, $\vec{G}_5^{\rm 6D} = (0, 2, -2, 4, 0, 4)$, one can see the diffuse scattering pattern that is observed around the origin, i.e., the hexagon in the 3f plane or the ring in the 5f plane. As seen in the 2f plane, the intensity of each vertex differs substantially, which makes the hexagon or the ring around $\vec{G}_5^{\rm 6D}$ slightly-distorted. There are exceptional patterns with which we cannot find intense reflections at their centers, such as a circle-like pattern at $\vec{Q}_{\rm HK} \sim (1.6, 0)$ Å^{-1} in the 3f plane, and a pentagon at $\vec{Q}_{\rm HK} \sim (0, 2.2)$ Å^{-1} in the 5f plane. Those patterns have slightly smaller diameters as compared to that appears around the origin, suggesting that they are satellites of out-of-plane reflections. We, in fact, found the Bragg reflections which are out of, but in vicinity of the planes, such as $\vec{G}_3^{\rm 6D} = (3, 1, 1, 1, 1, 1)$ for the circle-like pattern and $\vec{G}_6^{\rm 6D} = (3, 3, 3, 1, -1, 1)$ for the pentagon. They are projected to the center positions of the corresponding patterns in the 3f and 5f planes, which are indicated by white crosses in the figures. Further, satellites from $\vec{G}_3$ or $\vec{G}_6$ almost coincide with the position of the circle-like or pentagon-like pattern in the plane. Therefore, we suggest that the diffuse scattering appearing in the Zn-Mg-Ho quasicrystal can be regarded as satellites of intense Bragg reflections, and the modulation vector in the 3D reciprocal space is probably represented by $\vec{q}_{\rm m\parallel} = (0, 0.55, 0)$.

MODULATION VECTOR IN THE 6D RECIPROCAL LATTICE SPACE

The prominent feature which distinguishes the diffuse scattering in the quasicrystal from ordinary crystals is that the intensities of the $\pm\vec{q}_{\rm m\parallel}$ satellites of one Bragg reflection are substantially different. This suggests that the magnetic modulation vector is defined in 6D reciprocal lattice space, since in this case we have an additional term in intensity, the Fourier transform of window function $|W(\vec{Q}_\perp)|^2$, which generally differs for $\vec{Q}_\perp = \vec{G}_\perp \pm \vec{q}_{\rm m\perp}$. Further, $|W(\vec{Q}_\perp)|^2$ is a rapidly decreasing function of $|\vec{Q}_\perp|$, and thus a peak with small $|\vec{Q}_\perp|$ can have high intensity. In the observations, the satellites around the origin, $\vec{O}_\parallel + \{\vec{q}_{\rm m\parallel}\}$, appear most intensely. Thus, the perpendicular-space component of the satellites, $\vec{O}_\perp + \{\vec{q}_{\rm m\perp}\} = \{\vec{q}_{\rm m\perp}\}$, is most likely $\simeq 0$, i.e., $\vec{q}_{\rm m\parallel\perp} \simeq (0, 0.55, 0, 0, 0, 0)$. Otherwise, a satellite of another reflection, $\vec{G}^{\rm 6D} + \vec{q}_{\rm m}^{\rm 6D}$, may accidently have smaller perpendicular-space component, and appear as a much intense peak. We found that the most simple and commensurate vector in 6D reciprocal lattice bases that is projected into $\vec{q}_{\rm m\parallel\perp}$ is $\vec{q}_{\rm m}^{\,\rm 6D} = (\frac{3}{4}, 0, 0, \frac{1}{2}, \frac{3}{4}, \frac{1}{2})$.

The modulation vector was mostly determined from the positional information of the diffuse peaks around the origin and a few intense Bragg reflections. As concern the intensity, $\vec{q}_{\rm m}^{\,\rm 6D}$ is restricted only by the fact that the diffuse satellites around the origin are the most intense. Thus, it is still uncertain that the observed intensity distribution of the satellites of all the Bragg reflections can be reproduced by the modulation vector. To confirm the validity of the vector, we have to calculate the intensity of all the satellites, and compare the results with the observation. We, here, formulate the scattering intensity of the 6D spin correlations with the modulation $\vec{q}_{\rm m}^{\,\rm 6D}$ by applying the projection-method for the spin system on the 6D hypercubic lattice. Details will be published elsewhere [16].

The Fourier transform of spin correlations can be defined between spins on the 6D hypercubic lattice as

$$< S(\vec{Q}^{\rm 6D})S(-\vec{Q}^{\rm 6D}) >= \sum_{l,d}\sum_{l',d'} < S_{l,d}S_{l',d'} > \exp(-{\rm i}\vec{Q}^{\rm 6D}\cdot(\vec{R}_l^{\rm 6D}+\vec{d}^{\rm 6D})+{\rm i}\vec{Q}^{\rm 6D}\cdot(\vec{R}_{l'}^{\rm 6D}+\vec{d}'^{\rm 6D})). \quad (1)$$

$S_{l,d}$ denotes a spin operator of the d-th RE atom in the l-th unit cell. If the correlations are

well developed, we can approximate it as,

$$< S(\vec{Q}_{\parallel\perp})S(-\vec{Q}_{\parallel\perp}) >\propto \sum_{\vec{G}^{6\mathrm{D}}} |F_{\mathrm{S}}(\vec{Q}^{6\mathrm{D}} - \vec{q}_{\mathrm{m}}^{\,6\mathrm{D}})|^2 (L(\vec{Q}_{\parallel\perp} - \vec{q}_{\mathrm{m}\parallel\perp} - \vec{G}_{\parallel\perp}) + L(\vec{Q}_{\parallel\perp} + \vec{q}_{\mathrm{m}\parallel\perp} - \vec{G}_{\parallel\perp})), \tag{2}$$

where $F_{\mathrm{S}}(\vec{Q}^{6\mathrm{D}})$ is the structure factor defined in the 6D space. $L(\vec{Q}_{\parallel\perp})$ is a Fourier transform of a spatial decay of the spin correlations. It is assumed to be sufficiently sharp and localized at $\vec{Q} = 0$. Note that this becomes the delta-function for infinite correlation length. Since the shape of the spatial decay is unknown for the 6D spin system, we assume the trial function as a product of Lorentzians, $L(\vec{Q}_{\parallel\perp}) \propto \prod_{n=1}^{6} \gamma/(\gamma^2 + Q_{\parallel\perp n}^2)$. This corresponds to $\exp(-|R|/\gamma)$ decay of spatial correlations along each orthogonal axis in the parallel and perpendicular space.

The projected spin-correlation function in the 3D reciprocal space, which is directly related to the neutron scattering intensity, is written in terms of the 6D correlations as [16],

$$< S(\vec{Q}_{\parallel})S(-\vec{Q}_{\parallel}) >\propto |f(\vec{Q}_{\parallel})|^2 \int \mathrm{d}\vec{Q}_{\perp} \sum_{\substack{\vec{G}^{6\mathrm{D}} \\ \{\vec{q}_{\mathrm{m}}^{\,6\mathrm{D}}\}}} |F_{\mathrm{s}}(\vec{Q}^{6\mathrm{D}} - \vec{q}_{\mathrm{m}}^{\,6\mathrm{D}})|^2 L(\vec{Q}_{\parallel\perp} - (\vec{G}_{\parallel\perp} + \vec{q}_{\mathrm{m}\parallel\perp}))|W(\vec{Q}_{\perp})|^2, \tag{3}$$

where $f(\vec{Q}_{\parallel})$ is the Ho^{3+} form factor [21].

We performed the integration numerically with the experimentally-obtained $\gamma = 0.1$ Å^{-1}. The results are shown in Fig. 8. In the integration, we used a rather simple sphere-shaped window-function proposed by Ohno and Ishimasa [22], since it is only one existing model. As can be seen by comparing the figures with Fig. 7, the symmetry and relative intensity of the diffuse scattering are well reproduced by the calculation. In the 2f plane, the ratio of satellite intensities, such as at $\vec{G}_3 \pm (0, 0.55)_{HK}$ or at $\vec{G}_2 \pm (0, 0.55)_{HK}$, is in good agreement with the experimental results. The ridge-like appearance is almost reproduced. For the 3f and 5f plane, the circle-like patterns and pentagons can be seen in the calculations, which qualitatively agree with the experiments. Those correspondences strongly suggest the validity of the 6D magnetic modulation vector. We note that the qualitative features, such as intensity ratio of the satellites, are unchanged for a small variation in the window function. However, it may possibly affect the results quantitatively. Thus, for further quantitative discussion, detailed shape of window functions and window positions may be necessary. The single-crystal structure-analysis is now in progress [23].

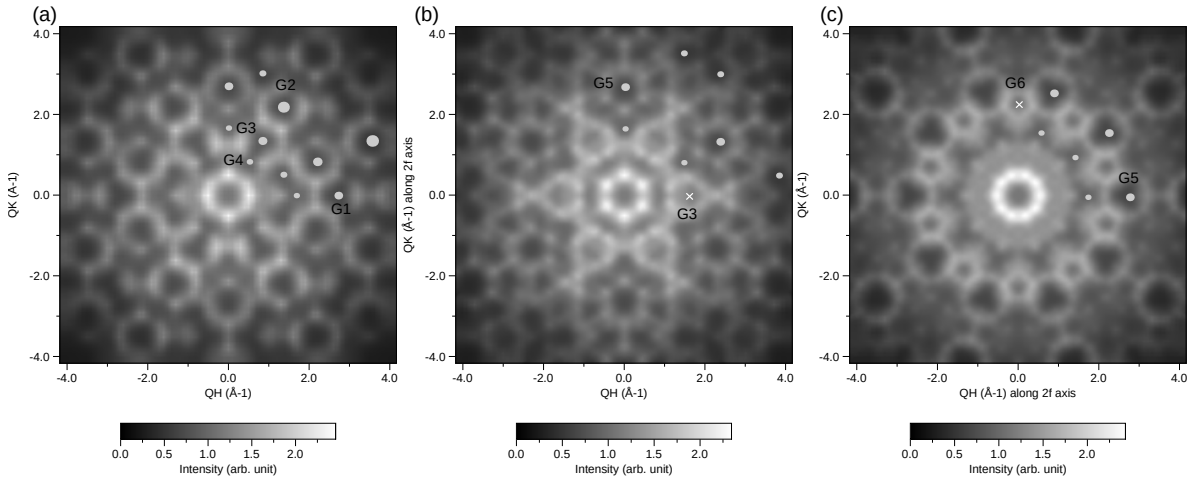

Figure 8: Results of calculation of the magnetic diffuse-scattering intensity for the (a) 2f, (b) 3f, and (c) 5f planes. White dots stand for the in-plane intense nuclear Bragg reflections in the first quadrant, whereas the white crosses are for the projected positions of the out-of-plane Bragg reflections, $\vec{G}_3^{6D}$ and $\vec{G}_6^{6D}$. Details are given in the text.

DISCUSSION AND CONCLUSIONS

In the previous report, we suggested the quasi-five-dimensional spin-correlations solely from the diffuse scattering ridges along the 5f axis, which appear in the 2f plane, as shown in the Fig. 7(a) [14]. However, from the viewpoint of the symmetry, this is somewhat questionable since the 6D lattice is cubic and has no uniaxial anisotropy. In this work, we have regarded the diffuse scattering as a set of rather localized peaks, which are satellites of the nuclear Bragg reflections. The magnetic modulation vector for the satellites was proposed as $\vec{q}_{\rm m}^{\,6D} = (\frac{3}{4}, 0, 0, \frac{1}{2}, \frac{3}{4}, \frac{1}{2})$. The calculation, performed with $\{\vec{q}_{\rm m}^{\,6D}\}$ and with γ being equal for all the axes, reproduced the observation qualitatively. This indicates that the spin correlations are rather 6D than the quasi-five-dimensional as suggested before. The diffuse ridges in the 2f plane originate from the fact that along the 5f axis there are a number of Bragg reflections which have relatively small $\vec{G}_\perp$, and thus the satellites can be observable almost continuously along the axis.

In the real space view, the validity of the 6D modulation vector indicates that the correlations develop between spins on the virtual 6D hypercubic lattice. This seems surprising since the real magnetic interactions should be defined in the real 3D space, although the structure is virtually defined in the 6D space. Further, the existence of well-developed correlations gives rise to another puzzling problem; why the susceptibility shows a typical spin-glass-like behavior, which is indicative of randomly frozen spins? Thus, a new type of magnetic order in the quasicrystal may be required to account the strong spin-correlations and random spin-glass-like behavior at once.

In conclusion, we have performed neutron scattering experiments on the powder and single crystalline Zn-Mg-Ho icosahedral quasicrystals, and on the powder of the related crystalline phase. The powder experiments revealed that only the diffuse scattering can be seen in the icosahedral quasicrystal. The previously-reported long-range order was assigned

to the crystalline contamination. The $\vec{Q}$ dependence of the diffuse scattering was measured in wide $\vec{Q}$ space on the 2f, 3f, and 5f planes. It shows that the magnetic diffuse scattering appears as satellites of the intense nuclear Bragg reflections. Further, by applying the projection-method to the spin system on the 6D hypercubic lattice, we have found that 6D spin correlations with the modulation vector of $\vec{q}_{\rm m}^{\rm 6D} = (\frac{3}{4}, 0, 0, \frac{1}{2}, \frac{3}{4}, \frac{1}{2})$ can reproduce the observation. The magnetic correlations are rather six-dimensional than previously-suggested quasi-five-dimensional. The relation between the well-developed short-range order and the random spin-glass-like behavior in susceptibility remains to be answered.

ACKNOWLEDGEMENTS

The present authors thank Drs. L. H. Tang and S. Matsuo for valuable discussions, and Drs. T. Ishimasa and B. Charrier for providing us the results prior to publication. This work is partly supported by CREST, Japan Science and Technology Corporation.

REFERENCES

[1] D. Shechtman, I. Blech, D. Gratias and J. W. Cahn, Phys. Rev. Lett. **53**, 1951 (1984).
[2] S. Matsuo, H. Nakano, T. Ishimasa and M. Mori, J. Phys. Soc. Jpn. **62**, 4044 (1993).
[3] M. A. Chernikov, A. Bernasconi, C. Beeli, A. Schilling and H. R. Ott, Phys. Rev. B **48**, 3058 (1993).
[4] T. Klein, C. Berger, D. Mayou and F. Cyrot-Lackmann, Phys. Rev. Lett. **66**, 2907 (1991).
[5] A. P. Tsai, A. Niikura, A. Inoue, T. Masumoto, Y. Nishida, K. Tsuda and M. Tanaka, Philos. Mag. Lett. **70**, 169 (1994).
[6] Y. Hattori, A. Niikura, A. P. Tsai, A. Inoue, T. Masumoto, K. Fukamichi, H. Aruga-Katori and T. Goto, J. Phys. Condens. Matter **7**, 2313 (1995).
[7] B. Charrier and D. Schmitt, J. Magn. Magn. Mater. **171**, 106 (1997).
[8] B. Charrier, B. Ouladdiaf and D. Schmitt, Phys. Rev. Lett. **78**, 1513 (1997).
[9] A. P. Tsai, A. Niikura, A. Inoue and T. Masumoto, J. Mater. Res. **12**, 1468 (1997).
[10] A. Langsdorf, F. Ritter and W. Assmus, Philos. Mag. Lett. **75**, 381 (1997).
[11] T. J. Sato, H. Takakura and A. P. Tsai, Jpn. J. Appl. Phys. **37**, L663 (1998).
[12] I. R. Fisher, Z. Islam, A. F. Panchula, K. O. Cheon, M. J. Kramer, P. C. Canfield and A. I. Goldman, Philos. Mag. B **77**, 1601 (1998).
[13] A. Langsdorf and W. Assmus, J. Cryst. Growth **192**, 152 (1998).
[14] T. J. Sato, H. Takakura, A. P. Tsai and K. Shibata, Phys. Rev. Lett. **81**, 2364 (1998).
[15] Z. Islam, I. R. Fisher, J. Zarestky, P. C. Canfield, C. Stassis and A. I. Goldman, Phys. Rev. B **57**, R11047 (1998).
[16] T. J. Sato *et al.*, in preparation.
[17] K. Ohoyama, T. Kanouchi, K. Nemoto, M. Ohashi, T. Kajitani, Y. Yamaguchi, Jpn. J. Appl. Phys. **37**, 3319 (1998).
[18] A. Yamamoto, Acta. Crystallogr. Sect. A **52**, 509 (1996).
[19] V. Elser, Phys. Rev. B **32**, 4892 (1985).
[20] M. L. Fornasini, J. Less-Common Met. **25**, 329 (1971).
[21] A. J. Freeman and J. P. Desclaux, J. Magn. Magn. Mater. **12**, 11 (1979).
[22] T. Ohno and T. Ishimasa, in *Proceedings of the 6th international conference on quasicrystals*, edited by S. Takeuchi and T. Fujiwara (World Scientific, Singapore, 1998) pp. 39-42.
[23] H. Takakura *et al.* to be submitted.